

Determination of the Texture Viscosity and Elasticity of a Nematic PBLG/d-DMF Solution through Magnetic Field Alignment

Norman J. Wagner* and Lynn M. Walker

Department of Chemical Engineering, University of Delaware, Newark, Delaware 19716

Received January 20, 1994; Revised Manuscript Received May 12, 1994*

ABSTRACT: A moderate magnetic field is used to align a polydomain, nematic sample of 16 wt % poly-(γ -benzyl L-glutamate) (PBLG) in deuterated *N,N*-dimethylformamide (d-DMF) orthogonal to a small-angle neutron scattering beam. The temporal evolution of the resultant domain alignment is analyzed through a molecular model for the scattering and a mean-field mechanical model. The latter includes both the viscous and elastic responses of the defect texture, which is responsible for the polydomain mesophase. The effective structure factor for the nematic phase is extracted from the SANS measurements, showing a reduction in scattering intensity that is presumed to arise from excluded volume interactions. We also extract a texture elasticity of 5×10^{-7} dynes for a texture size of $\approx 3 \mu\text{m}$ from the steady-state alignment, and a shear viscosity of 28 Pa s at a characteristic shear rate of $\approx 2 \times 10^{-4} \text{ s}^{-1}$ from the long-time temporal response. The latter is over 20 times the measured nematic viscosity and suggests a possible influence of the texture on the very low shear viscosity. The short-time temporal response is found to be in good agreement with predictions from nematodynamics.

I. Introduction

The viscoelastic response and architecture of the defect texture resident in lyotropic liquid crystalline polymers (LCPs) control aspects of the processing and final product performance of materials based on LCPs.¹ As opposed to the well-developed molecular theories for rheology and the structure of unidomain nematics of rodlike polymers,²⁻⁵ the supramolecular architecture and viscoelastic response of the defect texture are largely beyond prediction, although recent efforts at understanding this texture have been fruitful.⁶⁻¹¹ Necessary information includes a molecular description of the nematic fluid structure inside the "domain" (defined as a region of relatively uniform molecular alignment), a description of the topology and molecular disalignment in the core of the defects, and a theory or understanding of how the structure of this defect texture and the fluid's rheology are coupled.¹² In an attempt to provide clues for the first and third of these mysteries we have applied an old idea, magnetic alignment of the liquid crystal, with small-angle neutron scattering (SANS), to probe the dynamics of the defect texture. The work to be presented here is novel in that we operate at a magnetic field strength below that which is required to uniformly align the LCP, but just sufficient to slowly order the polydomain architecture without altering the defect texture itself. As the length scales probed by SANS are smaller than the characteristic size of the uniform fluid inside the defect texture, comparison of the SANS data with molecular models for the scattering yields information about the nematic structure inside the domains. Through the use of mean-field mechanism models, we are able to extract both the elasticity of the defect network and the characteristic fluid viscosity from the temporal evolution of the order parameter determined through SANS measurements.

II. Experimental Section

The polymer used in this study was purchased from Sigma Chemical Co. (Lot No. 109 F5501) and used without modification.

* To whom correspondence should be sent.

© Abstract published in *Advance ACS Abstracts*, September 1, 1994.

The manufacturer provides a molecular weight of 235 000 determined by LALLS. This corresponds to a rod length of 160 nm based on a monomer molecular weight of 219 and length of 0.15 nm. *N,N*-Dimethylformamide was used as a solvent because of its availability in deuterated form from Cambridge Isotope Laboratories. Although DMF is a good, helicogenic solvent which limits molecular aggregation, the polymer will precipitate from solution in the presence of even small amounts of moisture. To avoid water contamination, the polymer was dried under vacuum at 50 °C overnight, all sample preparation was performed in a dry nitrogen atmosphere, and samples were stored over desiccant.

A 15.8 wt % solution of PBLG in d-DMF was prepared by diluting a 30 wt % sample of PBLG in d-DMF. SANS experiments on the 30 wt % sample exhibited no aggregation, so the sample was diluted for use in this study. Samples were equilibrated at least 1 week prior to loading into SANS cells, which consisted of two quartz windows separated by a 1 mm thick brass spacer and enclosed in an aluminum holder. SANS experiments were performed on the 30 m instrument at NIST with the impinging neutron beam perpendicular to both the magnetic field and sample surface. All experiments were performed at 30 °C with an electromagnet providing a maximum 1 T field. Most of the temporal alignment experiments were performed with a neutron wavelength of 6 Å and a spread of 34.3%; otherwise a wavelength of 5 Å with a spread of 14.7% was used to more accurately determine absolute scattering properties, background corrections, and terminal alignment.

Rheological properties of the solutions were measured using a Bohlin controlled stress rheometer with cone and plate geometry. Texture size was determined through polarized microscopy on a drop of sample between a slide and coverslip. The characteristic texture size was determined by directly measuring the average traversal length from the photographs.¹³

III. Theory and Modeling

Following the suggestions in Kalus et al.,¹⁴ the scattering from suspensions of rods was simplified to extract information about the correlations in center of mass and orientation fluctuations. The basic assumptions applied to the exact model are as follows.

- The orientation of a rod is decoupled from all other particles, for all separations. Therefore,

$$\langle F(\mathbf{q}_j, \mathbf{u}_j) \rangle = \langle F(\mathbf{q}_j) \rangle \quad (1)$$

where F is the single rod scattering function, \mathbf{q}_j is the

scattering vector for rod j , and \mathbf{u}_j is the orientation vector along the rod axis.

- The center of mass pair correlation depends only on the relative distance $|\mathbf{r}|$ of separation.
- The particles are monodisperse in shape and scattering length density.

These assumptions lead to

$$I(\mathbf{q}) = C\phi V_p (\Delta\rho)^2 [\langle F^2(\mathbf{q}) \rangle + \langle F(\mathbf{q}) \rangle^2 h(q)] \quad (2)$$

Here, C accounts for instrument factors, ϕ is the volume fraction of rods of volume V_p , and $\Delta\rho$ is the scattering length density difference between rods and solvent. The function $h(q)$ characterizes the center of mass correlations between rods.

For particles that are strongly correlated orientationally, such that the nearest neighbors are nearly aligned, the second term is modified by replacing

$$\langle F(\mathbf{q}) \rangle^2 \rightarrow \langle F^2(\mathbf{q}) \rangle \quad (3)$$

which is exact in the limit of complete alignment. Thus,

$$I(\mathbf{q}) = C\phi V_p (\Delta\rho)^2 \langle F^2(\mathbf{q}) \rangle S_{\text{eff}}(q) \quad (4)$$

where $S_{\text{eff}}(q)$ is defined as the effective structure factor. As a result of these assumptions, the angular dependence of the scattering pattern arises totally from the form factor.

The form factor can be calculated for long rods directly from relations given in van de Hulst,¹⁵ where

$$F(\mathbf{q}, \mathbf{u}) = \sin(\mathbf{q} \cdot \mathbf{u}L/2) / (\mathbf{q} \cdot \mathbf{u}L/2)$$

The result of such a calculation for rods of length L that are randomly distributed with respect to orientation is

$$\langle F^2(q) \rangle = \frac{2}{qL} \int_0^{qL} \frac{\sin(\omega)}{\omega} d\omega - \left(\frac{\sin(qL/2)}{qL/2} \right)^2 \quad (5)$$

This result has been verified experimentally for PBLG/d-DMF systems in the dilute limit,¹⁶ which enables us to determine the prefactors in eq 4.

For the nematic phase, the ensemble average requires a distribution of rod orientations. In this work we will use the Maier-Saupe theory,⁵ which defines a reference potential for the excluded volume interactions between two rods as U_{ms} , yielding

$$f_{\text{N}}(\mathbf{u}) = \frac{1}{z} \exp(m(\mathbf{u} \cdot \mathbf{n})^2) \quad (6)$$

where z is the normalization constant and

$$m = \frac{3}{2} U_{\text{ms}} S_{\text{N}} / kT$$

$$S_{\text{N}} = \frac{3}{2} \mathbf{S}_{\text{N}} : \mathbf{nn}$$

$$\mathbf{S}_{\text{N}} = \int \left(\mathbf{uu} - \frac{1}{3} \mathbf{I} \right) f_{\text{N}}(\mathbf{u}) d\mathbf{u} \quad (7)$$

where \mathbf{n} is the director for the monodomain and subscript N denotes nematic (or molecular, to distinguish from the domain order parameter to follow). The solution of eq 7 then provides a self-consistent solution for the order parameter and the distribution function as a function of U_{ms}/kT . The form factor for a monodomain sample oriented along direction \mathbf{n} is then given by simple integration over this distribution.

For the textured material investigated here we will assume that as the length scale of the texture (typically tens of micrometers) is much greater than the length scales probed by neutron scattering ($\approx 1-100$ nm), the defect texture itself does not contribute to the SANS intensity. Therefore, the form factor can be calculated as

$$\langle \langle F^2(\mathbf{q}) \rangle_{\text{N}} \rangle_{\text{D}} \quad (8)$$

where subscript N denotes a nematic region and D denotes the domain orientations. We expect that the domains will be distributed about the field direction with a Gaussian distribution in angle as

$$f_{\text{D}}(\mathbf{n}) = \frac{1}{z_{\text{D}}} \exp(m_{\text{D}}(\mathbf{n} \cdot \mathbf{h})^2) \quad (9)$$

where \mathbf{h} is the field direction and z_{D} and m_{D} are the normalization and the interaction parameters for the domains, in direct analogy to the Maier-Saupe distribution. The order parameter associated with the domain orientation is therefore given by

$$S_{\text{D}} = \frac{3}{2} \mathbf{S}_{\text{D}} : \mathbf{hh}$$

$$\mathbf{S}_{\text{D}} = \int \left(\mathbf{nn} - \frac{1}{3} \mathbf{I} \right) f_{\text{D}}(\mathbf{n}) d\mathbf{n} \quad (10)$$

When the form factor for the polydomain nematic fluid is analyzed, the total form factor, as given by eq 8 above, is equivalent to averaging over a hypothetical monodomain of broader distribution. This is obvious when one considers that all inter-rod interference effects are buried in $S_{\text{eff}}(q)$ and that the form factor contains only intra-rod effects. Therefore, we need to relate this effective order parameter back to the true order parameters for the nematic fluid and the polydomain texture. In the following we assume that each domain region is of approximately the same size. Then the order parameter for the entire system is given by

$$S_{\text{m}} = \frac{3}{2} \mathbf{S}_{\text{m}} : \mathbf{hh}$$

$$\mathbf{S}_{\text{m}} = \int S_{\text{N}} f(\mathbf{n}) d\mathbf{n} \quad (11)$$

where subscript m denotes the measured order parameter. The molecular, or nematic, order parameter is given by eq 7 above and can be expressed in coordinates natural to each director \mathbf{n} as

$$\mathbf{S}_{\text{N}} = \left\langle \cos^2 \theta - \frac{1}{3} \right\rangle_{\text{N}} \left(\mathbf{nn} - \frac{1}{3} \mathbf{I} \right) + \langle \sin^2 \theta \rangle_{\text{N}} (\mathbf{I} - \mathbf{nn}) \quad (12)$$

where $\cos \theta = \mathbf{u} \cdot \mathbf{n}$ and $S_{\text{N}} = (3/2) \langle \cos^2 \theta - 1/3 \rangle_{\text{N}}$. Then, the domain average becomes (rotating the axis of each nematic-based coordinate frame into alignment with the Cartesian system defined by the field)

$$\mathbf{S}_{\text{m}} = \left\langle S_{\text{N}} \left(\cos^2 \theta - \frac{1}{3} \right) \right\rangle_{\text{D}} \left(\mathbf{hh} - \frac{1}{3} \delta \right) + \text{orthogonal terms} \quad (13)$$

This equation is readily integrated, as S_{N} is a constant for all the domains, yielding

$$\begin{aligned} S_{\text{m}} &= \frac{3}{2} \mathbf{S}_{\text{m}} : \mathbf{hh} \\ &= S_{\text{N}} S_{\text{D}} \end{aligned} \quad (14)$$

The above constitutes proof that, for a relatively uniform size distribution of uniaxial nematic domains where the domains are distributed in a uniaxial and Gaussian manner about the field direction, the measured order parameter from the form factor is indeed the product of the nematic and domain order parameters. This result agrees with that proposed by Picken et al.,¹⁷ which was based on the more general analysis of the rotational properties of the irreducible tensor components of the order tensor by Zannoni.¹⁸ A tensorial version of this result was postulated by Larson and Doi⁶ and has been used by others¹¹ to study nematics under shear flow; however, it is not apparent from either the above or the more general approach that the simple tensorial generalization should hold. Nonetheless, for the magnetic field alignment of uniaxial domains, the total parameter can be deconvoluted from the domain contribution if the molecular or nematic order is known.

A. Mechanical Model. The application of a magnetic field couples to the diamagnetic susceptibility of the rodlike PBLG macromolecules, which is positive and aligned with the long axis of the helix.¹⁹ The nematic “domains” are anchored, however, to the defect texture and, presumably, to the walls of the cell. The resulting competition between the elasticity of twisting the nematic and the magnetic torque gives rise to the concept of a nematic coherence length $\xi(H)$, defined in terms of the diamagnetic susceptibility χ , the applied field H , and the Frank elastic constant K (in the one constant approximation) as²

$$\xi(H) = \left(\frac{K}{\chi}\right)^{1/2} \frac{1}{H} \quad (15)$$

If the magnetic coherence length is significantly less than the size of a typical “domain”, then we would expect the nematic to form a uniformly aligned unidomain in the direction of the field—as would be the case for large applied fields.

As we will show, for the system under consideration the field is adjusted such that the magnetic coherence length is approximately equal to the size of the domain. Under these conditions, the basic architecture of the defect texture is expected to be unaffected by the applied field other than to tend to align each individual “domain” preferentially along the field axis. Further, the detailed molecular structure inside the “domain” will be unaffected by the field. Therefore, the physical picture is of the cooperative alignment of the domains due to the torque induced on each domain (thought of as a rigid body). This torque is resisted by the viscous nature of the defect ridden fluid and the elasticity associated with the defect texture. The final degree of alignment will be given by a balance of the characteristic magnetic torque against the latter, while the time evolution of the order parameter characterizing the net domain alignment will be governed by the former.

As the detailed architecture of the defect texture has not been adequately quantified such that exact calculations would be feasible, we pursue a more phenomenological approach founded in physical intuition that permits extraction of the two mechanical parameters of interest: the elastic constant and viscosity of the defect texture. There is significant mechanical and rheo-optical evidence^{10,20–24} for the existence of “domains”, as also deduced from electron microscopy.²⁵ Although a somewhat artificial construct, these domains, which consist of a characteristic length scale set by the density of defects in the texture, are a useful concept for understanding the complex viscoelastic response of textured LCPs.^{6,7,26} In what follows, we track the evolution of an ensemble of

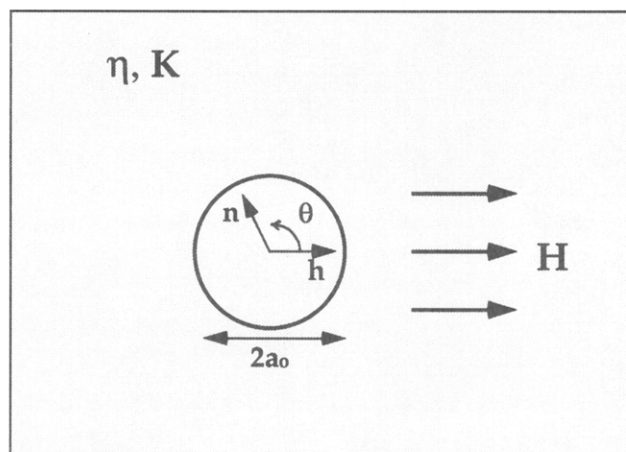


Figure 1. Nematic “domain” of size a_0 with director \mathbf{n} embedded in a fluid of viscosity η and elasticity K , subject to field H along direction \mathbf{h} .

domains embedded in a mean-field fluid with characteristic viscosity η and elastic constant (in the one-constant approximation) K . This will lead to an evolution equation for the order parameter of the domain alignment $S_D(t; \eta, K)$ that is of the form of a driven Voigt element.

Imagine a single domain, which will be taken as a sphere of radius a_0 , embedded in a fluid with elasticity K and viscosity η (see Figure 1). The torque acting on the domain due to the applied field is given by

$$T^M = \mu_0 \chi \left(\frac{4\pi a_0^3}{3}\right) \cos(\theta) \sin(\theta) H^2 \quad (16)$$

where θ is the angle between the field direction and the nematic director. Opposing this torque will be the linear elasticity associated with rotating the sphere toward the field and distorting the elastic network. For linear elastic behavior, the opposing torque will be given in terms of the displacement in orientation $\delta\theta$ as

$$T^K = -8\pi \left(\frac{K}{a_0^2}\right) a_0^3 \delta\theta \quad (17)$$

If only the final state of the sample were of interest, the resultant average angle would yield the final order parameter induced by the field. However, the temporal response will be dictated by balancing the difference between these two against the viscous drag on the domain. For Stokes flow, the frictional torque is given by

$$T^\eta = -8\pi \eta a_0^3 \frac{\partial\theta}{\partial t} \quad (18)$$

As the sum of the torques must be zero, we find

$$T^\eta + T^K = T^M$$

$$8\pi \eta a_0^3 \frac{\partial\theta}{\partial t} + 8\pi \left(\frac{K}{a_0^2}\right) a_0^3 \delta\theta = \mu_0 \chi \frac{4\pi a_0^3}{3} \cos(\theta) \sin(\theta) H^2 \quad (19)$$

To track the order parameter for the domains, defined by eq 10, eq 19 is multiplied by $\cos(\theta) \sin(\theta)$ and ensemble averaged. Using the standard decoupling approximation of Doi³ that $\langle \cos^4(\theta) \rangle = (1/9)(2S + 1)^2$ immediately yields

$$3\beta^{-1} \frac{\partial S_D}{\partial t} + \alpha S_D = -2S_D^2 + S_D + 1 \quad (20)$$

$$\alpha = \frac{18(K/a_0^2)}{\mu_0 \chi H^2} \quad (21)$$

$$\beta = \frac{\mu_0 \chi H^2}{6\eta} \quad (22)$$

The analytical solution to this equation is obtained by defining $\gamma \equiv S + (1/2)(3\alpha - 1)$, separating variables, and integrating to yield

$$\frac{1}{2} \ln \left[\frac{\sqrt{\Gamma} + \gamma}{\sqrt{\Gamma} - \gamma} \right] = \frac{2}{3} \beta t \quad (23)$$

$$\Gamma = \frac{\sqrt{3}}{2} \sqrt{(3\alpha^2 - \alpha + 1)}$$

where the boundary condition $S_D(t=0) = 0$ was used. Therefore, a semilog plot of the left-hand side of eq 23 against time yields the value of the viscosity, once the elasticity has been determined from the final degree of alignment.

Another possible interpretation of our magnetic field alignment experiments is provided by the equations of nematodynamics.² In the more traditional experiment on a homogeneous nematic with wall anchoring, a torque balance yields

$$\gamma_1 \frac{\partial \theta}{\partial t} + K' \frac{\partial^2 \theta}{\partial z^2} = \mu_0 \chi \cos(\theta) \sin(\theta) H^2 \quad (24)$$

Here, γ_1 is the rotational viscosity and K' (with the prime to distinguish that it is derived from the above equation, as opposed to eq 19 above) is taken as the Frank elasticity in the one-constant approximation. For small displacements, the second derivative scales as $\approx \delta\theta/a_0^2$; therefore we essentially recover an equation similar in form to eq 19 above, but the physical picture is rather different. In the nematodynamics approach, which is constrained to weak gradients in director orientation, the nematic director is twisted by the field where the initial, anchored director orientation does not lie along the field direction. In the "domain" view presented above, the nematic fluid itself remains intact, but the domains themselves orient with the field. The major difference comes in the identification of the viscosity appearing in eqs 19 and 24 above. The domain model identifies the viscosity as that of the fluid consisting of defect texture and nematic fluid, while the nematodynamics approach clearly identifies the viscosity as the rotational viscosity of the nematic. We note that previous work by Filas²⁷ used the same equation without Frank elasticity to successfully analyze the magnetic realignment of PBG/dichloromethane nematic monodomains.

To extract the *nematic* rotational viscosity and elasticity from the nematodynamic torque balance, we notice that the following mapping results in the same equation as eq 19 above:

$$\begin{aligned} \gamma_1 &\rightarrow 6\eta \\ K' &\rightarrow 6K \end{aligned} \quad (25)$$

Thus, either set of parameters may be extracted from the experiment depending upon the appropriate physical picture.

IV. Results

Graphical results for the observed alignment under magnetic fields are shown in Figure 2. As loaded (a), the

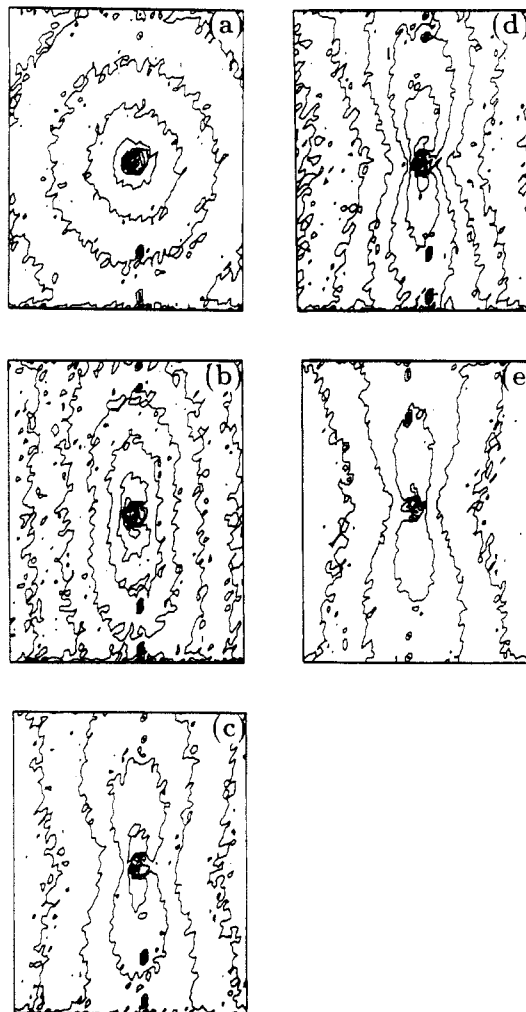


Figure 2. Contour plots of measured scattered intensity for 16 wt % PBLG/d-DMF for (a) starting sample, (b) 10 min, (c) 20 min, (d) 30 min, and (e) 60 min. The linear dimensions ($1/2$ of the box length) correspond to $qL = 288$. Note that the field direction is horizontal.

sample is seen to exhibit a circularly symmetric pattern indicative of negligible domain ordering. Upon application of the magnetic field ordering was observed. As seen, there is a strong degree of order along the field direction, as evidenced by the "hourglass" pattern, oriented perpendicular to the field direction. The total time to steady alignment was approximately 1 h. These data were obtained by taking averages over 10 min slices for the first 60 min, and 1 h slices thereafter. The sample was allowed to relax upon cessation of the field. After approximately 3 h the sample was observed to have recovered almost to the isotropic pattern seen initially.

Analysis of these patterns proceeded by attempting to capture the anisotropy through the form factor, as suggested by eq 4. However, as there is no robust method of estimating the full scattering intensity for such anisotropic hard rods, we proceed by using eq 4 to determine, experimentally, the value of $S_{\text{eff}}(q)$, where we use our previous results for dilute solutions of PBLG/d-DMF to fix all the experimental parameters (scattering length density difference, rod length, rod diameter, and incoherent background). The value of $S_{\text{eff}}(q)$ determined from this procedure is shown in Figure 3, where it is seen that the excluded volume effects reduce the scattering intensity, leading to $S_{\text{eff}}(q) < 1$. The consistency through all data sets of $S_{\text{eff}}(q)$ indicates that the ansatz of no orientation-center-of-mass coupling is correct. Therefore, our tech-

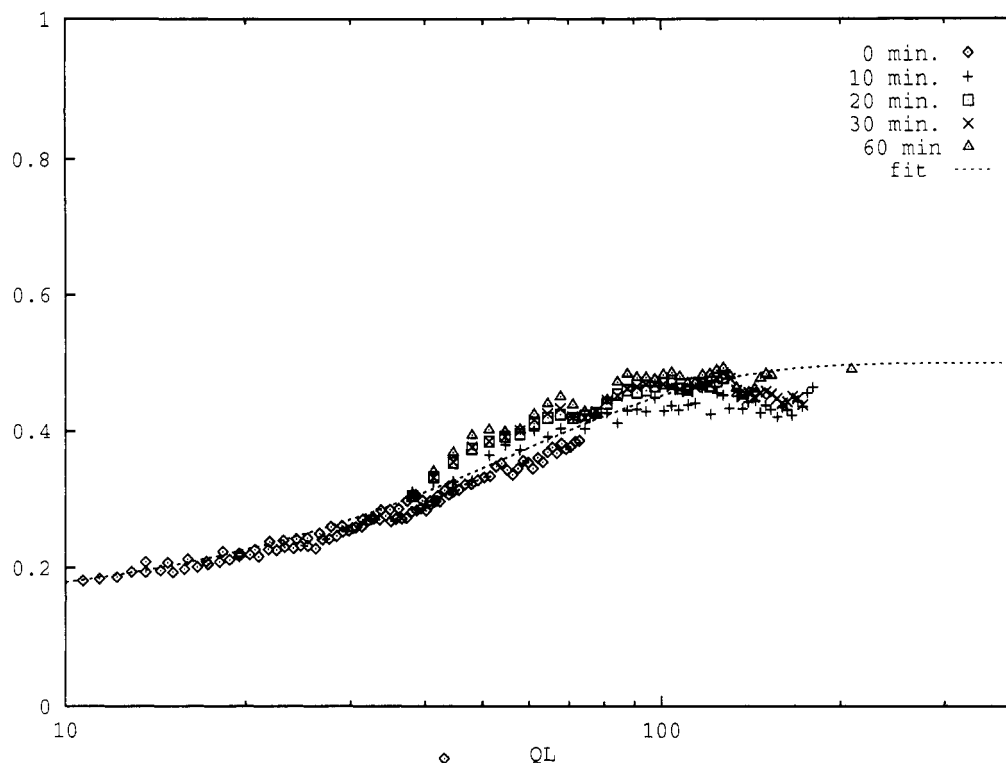


Figure 3. $S_{\text{eff}}(q)$ versus qL . The data correspond to the plots shown in Figure 2. The line is an empirical best fit; see text.

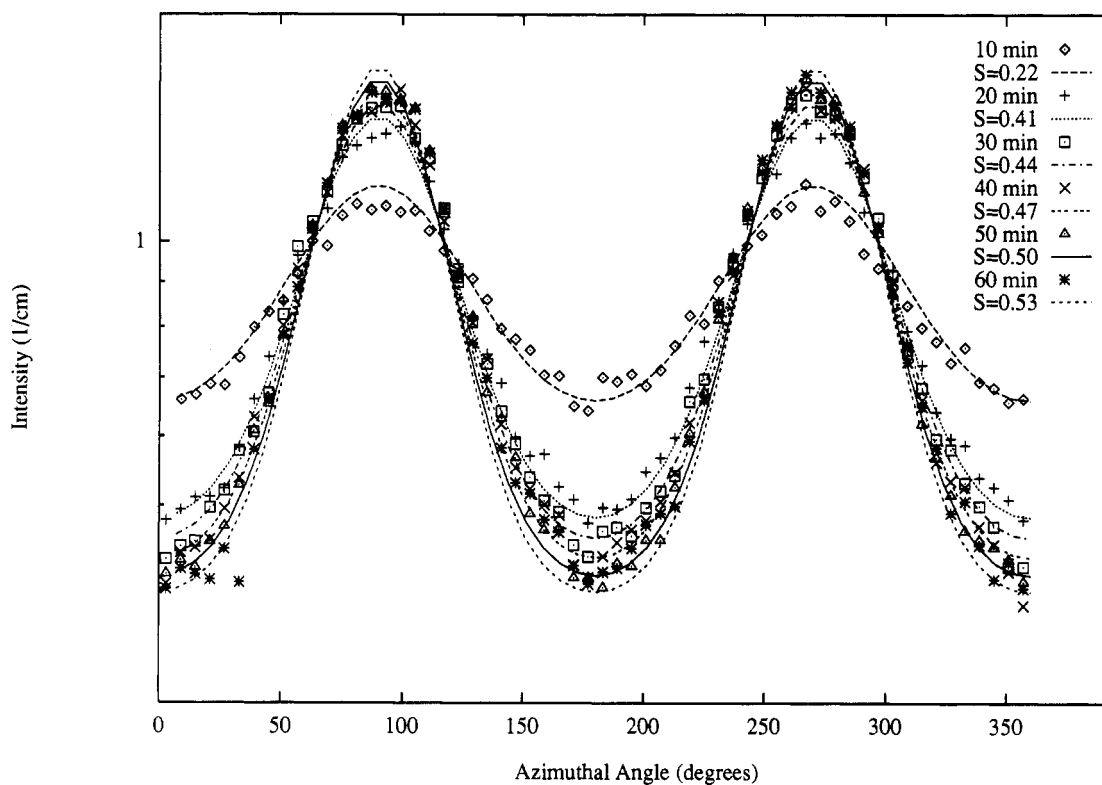


Figure 4. Plots of the azimuthal angular dependence of the scattering intensity at $qL = 80$ compared to the theoretical fits, as labeled.

nique for extracting the domain order parameter is also consistent and correct. For later fitting purposes, the function $S_{\text{eff}}(q) = 0.13 + 0.37 \tanh(qL/75)$ was empirically determined to accurately represent the data in this range.

This then enables the precise determination of S_m , the total or measured order parameter from the angular dependence of the form factor. We used the above values for the scattering parameters and structure factor to evaluate the angular dependence of the SANS patterns at $q = 0.5 \text{ nm}^{-1}$ (or $qL = 80$). The fits to the data are shown

in Figure 4, and the derived order parameters are shown in Table 1. The resulting predictions for the intensity are shown in Figure 5, where the fit and measured intensities (Figure 2) are to be compared. The results validate the assumptions underlying the simplified expression, eq 4.

To extract the domain order parameter, we use the value of $S_N = 0.8$ determined from interpolation of the data of Abe and Toshimasa,²⁸ which was obtained on a similar molecular weight polymer through the use of NMR. This value is very reasonable for the nematic at such concen-

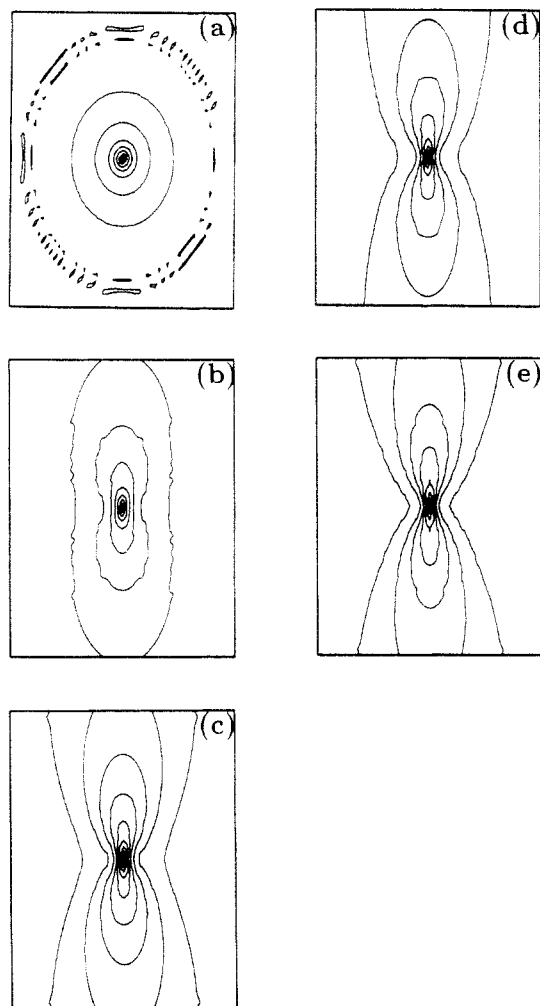


Figure 5. Theoretical fits of the scattering intensity. Labels and dimensions are the same as in Figure 2.

Table 1. Evolution of the Measured and Domain Order Parameters

time (min)	S_m	S_D	time (min)	S_m	S_D
0	0	0	40	0.47	0.59
10	0.22	0.28	50	0.50	0.62
20	0.41	0.51	60	0.53	0.66
30	0.44	0.55	480	0.56	0.70

trations above the isotropic-nematic transition. The resultant domain order parameter is also shown in Table 1. It is clear that alignment of the domains is not complete under this 1 T field, which enables us to determine both the characteristic elastic and viscous constants from the above experiment.

Balancing the field against the texture elasticity, the steady-state solution of eq 20 above yields

$$\alpha S_D = -2S_D^2 + S_D + 1 \quad (26)$$

The solution for the quadratic is

$$S_D = \frac{1}{4}((1 - \alpha) \pm \sqrt{\alpha^2 - 2\alpha + 9}) \quad (27)$$

For $S_D = 0.7$, $\alpha \approx 1$, which demonstrates that the field and texture elasticity are comparable for this sample. From eq 21 the texture elasticity is calculated to be

$$\frac{K}{\alpha_o^2} = \frac{\mu_o \chi H^2}{18} \quad (28)$$

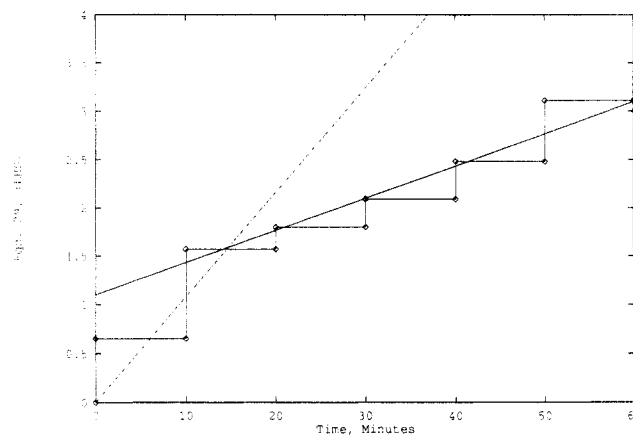


Figure 6. Plot of the left-hand side of eq 29 versus time. (\diamond) are the SANS results (represented as 10 min averages). The dotted line is the short time or initial slope, and the solid line is the best fit for long times.

The accepted value for χ , the diamagnetic susceptibility, for PBLG in organic solvents is $6.8 (\pm 0.7) \times 10^{-9} \text{ emu/cm}^3$ (on a per volume basis^{19,29}). Calculation for the 10K Oersted applied field yields $K/\alpha_o^2 = 0.039 \text{ dynes/cm}^2$ (0.0039 Pa).

In terms of the order parameter, the governing equation of $\alpha = 1$ is

$$\ln \left[\frac{\sqrt{1/2 + S_D/\sqrt{5}}}{\sqrt{1/2 - S_D}} \right] = \frac{4}{3} \beta t \quad (29)$$

Thus, a rather simple exponential decay is obtained for the ratio containing only the domain order parameter. A semilogarithmic plot of this relation is shown in Figure 6, which shows good agreement with the above relation except for short times. As the data are averages over 10 min slices, the plot shows a step representation of the results. As the initial sample alignment is expected to be sensitive to details of the domain polydispersity and other phenomena neglected in the above expressions, we choose to, for the moment, ignore the initial 10 min of response and fit only the region exhibiting the predicted linear behavior. The best fit line yields a value of $\beta = 4.2 \times 10^{-4}$. This yields a value for the viscosity of

$$\begin{aligned} \eta &= \frac{\mu_o \chi H^2}{6\beta} \\ &= 28 \text{ Pa s} \end{aligned}$$

Our viscosity measurements on this sample in the region II plateau showed stable values of 1.1 Pa s for shear rates around 1 s^{-1} . This value for the plateau shear viscosity is consistent with previous work²³ on PBLG in *m*-cresol if the differences in solvent viscosity are accounted for. Yet our experimentally derived viscosity from the magnetic alignment is significantly higher than the plateau viscosity of the nematic fluid.

This viscosity may be interpreted as the rotational viscosity appearing in the continuum theory presented previously (eq 24). Using the molecular theory of Doi and Edwards³ for relating the nematic rotational viscosity γ_1 and plateau shear viscosity, η_{II} (where the subscript denotes the region II viscosity) to the order parameter enables us to predict this value from the measured rheology. For a nematic order parameter of 0.8, this yields $\gamma_1 = 35 \eta_{II}$. Thus, we expect a rotational viscosity on the order of $\approx 40 \text{ Pa s}$. Remembering the factor of 6 between the rotational viscosity (see eq 25) and the effective texture viscosity,

our measurement yields a value of 170 Pa s for the former. Thus, the nematic theory predicts a rotational viscosity that is significantly lower than what is observed over the course of alignment, and hence, it is not possible to interpret the long-time results of our experiment directly in terms of the nematodynamics theory. However, if the picture that the nematic fluid in any "large" domains will indeed rotate and align with the field before large scale realignment of the domains themselves is correct, then the *initial* slope should be more representative of this continuum picture. The initial slope plotted in Figure 6 yields a value of $\beta = 1.33 \times 10^{-3}$, which gives a rotational viscosity of 53 Pa s. This is rather remarkable agreement with the above calculation, especially given the approximations therein. Thus, the presumed picture that any material contained in "large" domains will initially rotate according to nematodynamics appears to be consistent with the measurements. However, this cannot account for the order of magnitude larger viscosity observed once this initial stage is nearly complete.

Previous work on magnetic reorientation of initially aligned samples of PBG in dichloromethane²⁷ observed excellent agreement with eq 24 without including any elasticity. However, for reorientations above a critical angle, discrepancies were found whereby the reorientation proceeded by a more rapid rate. This was attributed to the counterrotation of some fraction of the polymer, resulting in a yielding-like behavior and the formation of defects in the fluid. Our SANS results on polydomain samples have the opposite deviation from eq 24, suggesting a different physical picture, such as the rotation of entire domains, must dominate the alignment process.

One possible interpretation of this increased viscosity is region I behavior, as originally proposed by Asada, Onogi, and co-workers.^{23,30} In region I the presence of defects is thought to yield a shear-thinning behavior that limits to the region II plateau as the shear stress exceeds the characteristic stress of the texture. In previous work the concept of a critical Ericksen number has been used to characterize the arresting of domain tumbling^{10,12} and to explain the evolution of texture in region I flows. Using this to obtain a characteristic shear rate for our experiment shows

$$Er = \frac{\eta \dot{\gamma}}{(K/a_0^2)} \quad (30)$$

$$Er \approx 1$$

$$\dot{\gamma} \approx 2 \times 10^{-4} \text{ s}^{-1}.$$

The onset of region I behavior $\dot{\gamma}_{I-II}$ has been postulated to be a strong function of the polymer concentration and the domain size,⁷ scaling for a particular solution as

$$\dot{\gamma}_{I-II} \approx \frac{1}{a_0^2} \left(\frac{\phi}{\phi_c} \right)^2 \quad (31)$$

Therefore, using recent³¹ and previous^{23,32} work on the rheology of PBLG/*m*-cresol nematics, the values obtained here for the viscosity and characteristic shear rates are at least in qualitative accordance with expectation. However, one must be cautioned that this value of the "viscosity" is highly subject to the model employed and is undoubtedly a transient value. Nonetheless, these results of the magnetic alignment experiment are provocative in that, subject to the above interpretation, the experiment demonstrates the existence of a region I rheology at

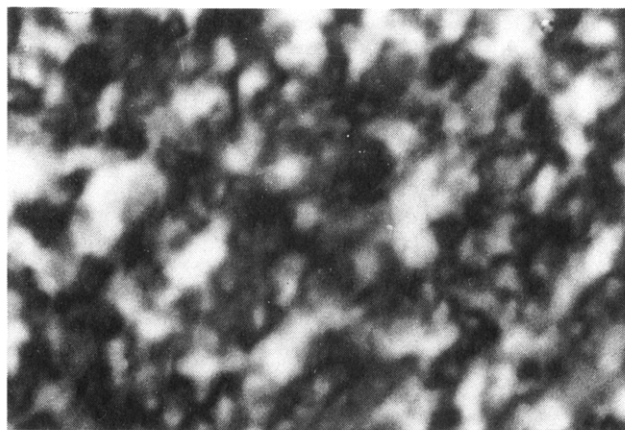


Figure 7. Texture of the PBLG/d-DMF solution under crossed polarizers at rest (no field).

polymer concentrations significantly lower than ever observed in mechanical measurements. We note that increasing the polymer concentration to 30 wt % results in a texture elasticity too stiff to be aligned by our magnetic field ($\alpha \ll 1$), in accordance with the above scaling.

We have also qualitatively observed the relaxation of our sample upon cessation of the magnetic field. For recovery of the Voigt element a single exponential decay with characteristic time constant $\alpha\beta/3$ is predicted. Therefore, the critical relaxation time for the domain order parameter is about 2 h, over which the measured order parameter should drop to about $S_m \approx 0.2$. Qualitatively, we observe that significant recovery was obtained after 2 h, with the sample appearing fully isotropic after 8 h, in good agreement with the Voigt element model.

Finally, we need to check the assumption that the domains remain intact during the course of alignment once the initial transient regime is past. Using the above relations we determine the magnetic coherence length from eq 15 as

$$\begin{aligned} \xi(H) &= \left(\frac{K}{\chi} \right)^{1/2} \frac{1}{H} \\ &= \frac{a_0}{H} \left(\frac{K/a_0^2}{\chi} \right) \\ &= \frac{a_0}{H} \left(\frac{\mu_0 \chi H^2}{18\chi} \right)^{1/2} \\ &= \frac{a_0}{3\sqrt{2}} \end{aligned} \quad (32)$$

where the value of $\alpha = 1$ has been used. Thus, we ensured that as long as the field balances the texture elasticity, the domain will remain a coherent magnetic unit, validating our assumption. Further, the magnetic field will distort the nematic director in any domains significantly larger than the coherence length (for which $\alpha \ll 1$) and, thus, attempt to create more defects. As this rotational viscosity is low relative to the "texture" viscosity and the directors are "pinned" by the texture, this process proceeds initially and should dominate the initial response of the nematic. The longer transient response should be dominated by the rotation of domains with the field, without altering the characteristic domain size.

To extract the Frank elasticity K , the characteristic domain size a_0 was measured as 36 μm using polarized optical microscopy. A typical "relaxed" domain structure is shown in Figure 7, where the shades denote different

domain optical thicknesses and orientations of the nematic director relative to the crossed polarizers. This size is in agreement with typical mesophase structural sizes observed in previous studies.³³ Using this value as a characteristic domain size, we determine that $K = 5 \times 10^{-7}$ dynes.

Theoretical predictions and bounds for this domain elasticity are available for testing this derived experimental value. Marrucci and Greco³⁴ derived values for the three Frank elastic constants for rodlike nematics in the Maier-Saupe approximation. As our material will yield along the easiest mode, we compute an absolute lower bound from their work as

$$K_{lb} \approx \nu k T P L^2 M \quad (33)$$

where ν is the number density of rods of length L , and P and M are given in the paper for our value of the order parameter as $P \approx 0.45$ and $M \approx 0.05$. For our rods the lower bound is computed to be $K_{lb} \approx 0.5 \times 10^{-7}$ dynes. As an upper bound, the value of our one-constant elasticity should be closest to that of the weakest Frank elastic constant, the twist elasticity K_{22} . Sridhar et al.²⁹ measured $K_{22} = 58.2 \times 10^{-7}$ dynes for a monodomain of 25.5 wt % solution of PBLG in dichloromethane. As the polymer had roughly twice the molecular weight (550K) as ours and is almost twice as concentrated, the scaling in eq 31 above suggests that our system should have a value almost 1 order of magnitude smaller—exactly as is derived from our measurements.

V. Conclusions and Summary

We have demonstrated a new application of magnetic field alignment with *in situ* SANS to probe the dynamics of the defect texture and to extract the effective structure factor of lyotropic nematics. The simplified scattering description can model the data quite well and yields an effective structure factor that exhibits suppressed scattering, probably due to excluded volume interactions. By balancing the applied field to the elasticity of the defect texture and monitoring the gradual alignment of the nematic domains without coalescing the domains with high field strengths, we have shown how the technique can be used to extract the overall and domain order parameters. The short-time response is governed by nematodynamics, corresponding to alignment of the nematic fluid contained within domains larger than the magnetic coherence length. A simple mechanical balance of the texture elasticity, viscosity, and magnetic field coupling is able to model the observed long-time alignment response. The numerical values extracted for the domain elasticity are in agreement with expectations based on previous measurements and theory. The resolved texture viscosity suggests that even this relatively low concentration nematic could exhibit region I behavior at low enough shear rates—shear rates significantly lower than those usually probed in rheological experiments on LCPs.

Acknowledgment. We gratefully acknowledge the help and consultation of Boualem Hammouda of NIST with these SANS measurements. Further, we acknowledge

reviewer's comments that led to linking the short-time response to nematodynamics. This work was supported under NSF Grant CTS-9158146 and by duPont Polymer Technology. This material is based upon activities supported by the National Science Foundation under Agreement No. DMR-9122444. We acknowledge the support of the National Institute of Standards and Technology, U.S. Department of Commerce, in providing the facilities used in this experiment.

References and Notes

- (1) Commission on Engineering National Research Council, National Materials Advisory Board and Technical Systems. *Liquid Crystalline Polymers*; National Academy Press: Alexandria, VA, 1990.
- (2) de Gennes, P.; Prost, J. *The Physics of Liquid Crystals*; 2nd ed.; Clarendon Press: Oxford, U.K., 1993.
- (3) Doi, M.; Edwards, S. F. *The Theory of Polymer Dynamics*; Clarendon Press: Oxford, U.K., 1986.
- (4) Larson, R. *Constitutive Equations for Polymer Melts and Solutions*; Butterworths: New York, 1988.
- (5) Chandrasekhar, S. *Liquid Crystals*; 2nd ed.; Cambridge University Press: Cambridge, U.K., 1992.
- (6) Larson, R. G.; Doi, M. *J. Rheol.* **1991**, *35* (4), 539.
- (7) Walker, L. M.; Wagner, N. J. *J. Rheol.*, in press.
- (8) Marrucci, G.; Maffettone, P. L. *J. Rheol.* **1990**, *34* (8), 1231.
- (9) Marrucci, G. *Pure Appl. Chem.* **1985**, *57* (11), 1545.
- (10) Burghardt, W. R.; Fuller, G. G. *J. Rheol.* **1990**, *34* (6), 959.
- (11) Hongladarom, K.; Burghardt, W. R.; Baek, S. G.; Cementwala, S.; Magda, J. *J. Macromolecules* **1993**, *26*, 772.
- (12) Marrucci, G.; Greco, F. *Advances in Chemical Physics*; Prigogine, I., Rice, S., Eds.; Wiley: New York, 1993.
- (13) Stein, R. S. *Polymer Blends*; Paul, D. R., Newman, S., Eds.; Academic Press: New York, 1978; Vol. 1, pp 393-442.
- (14) Kalus, J.; Hoffmann, H.; Ibel, K. *Colloid Polym. Sci.* **1989**, *267*, 818.
- (15) van de Hulst, H. C. *Light Scattering by Small Particles*; Dover: New York, 1957.
- (16) Wagner, N. J.; Walker, L. M.; Hammouda, B. Submitted for publication in *Macromolecules*.
- (17) Picken, S. J.; Aerts, J.; Doppert, H. L.; Reuvers, A. J.; Northolt, M. G. *Macromolecules* **1991**, *24*, 1366.
- (18) Zannoni, C. In *The Molecular Physics of Liquid Crystals*; Luckhurst, G. R., Gray, G. W., Eds.; Academic Press, London, 1979; p 51.
- (19) Sridhar, C. G.; Hines, W. A.; Samulski, E. T. *J. Chem. Phys.* **1974**, *61* (3), 947.
- (20) Wissbrun, K. F. *Br. Polym. J.* **1980**, Dec, 1963.
- (21) Marrucci, G. *Rheol. [Proc. Int. Congr.]* **9th** **1984**, 441.
- (22) Asada, T.; Onogi, S.; Yanase, H. *Polym. Eng. Sci.* **1984**, *24* (5), 355.
- (23) Asada, T.; Tanaka, T.; Onogi, S. *J. Appl. Polym. Sci., Appl. Polym. Symp.* **1985**, *41*, 229.
- (24) Takebe, T.; Hashimoto, T.; Ernst, B.; Navard, P.; Stein, R. *J. Chem. Phys.* **1990**, *92* (2), 1386.
- (25) Thomas, E. L.; Wood, B. A. *Faraday Discuss. Chem. Soc.* **1985**, *79*, 299.
- (26) Larson, R. G.; Mead, D. W. *J. Rheol.* **1989**, *33*, 1251-1281.
- (27) Filas, R. W. *Mesomorphic Order in Polymers*; Blumstein, A., Ed.; page 157. ACS Symposium Series; American Chemical Society: Washington, DC, 1978.
- (28) Abe, A.; Yamazaki, T. *Macromolecules* **1989**, *22*, 2145.
- (29) Sridhar, C. G.; Hines, W. A.; Samulski, E. T. *J. Phys., Colloq.* **1975**, 269.
- (30) Asada, T.; Muramatsu, H.; Watanabe, R.; Onogi, S. *Macromolecules* **1980**, *13*, 867.
- (31) Walker, L. M.; Wagner, N. J.; Larson, R.; Moldenaers, P. *J. Rheol.* to be submitted for publication.
- (32) Kiss, G.; Porter, R. S. *J. Polym. Sci., Polym. Phys. Ed.* **1980**, *18*, 361.
- (33) Gleeson, J. T.; Larson, R. G.; Mead, D. W.; Kiss, G.; Cladis, P. E. *Liq. Cryst.* **1992**, *11*, 341.
- (34) Marrucci, G.; Greco, F. *Mol. Cryst. Liq. Cryst.* **1991**, *206*, 17.